

Please find below the referee 2 comments (in black) and our answers (in blue).

**Anonymous Referee #2**

L183+196: This equality is only approximate (to 1. order), right? Perhaps use a  $\simeq$ .

Ok, done. See lines 183-196

L242-3: "changes in clear-sky radiation changes". One too many "changes".

Ok, done. The second "changes" is deleted from the text. See line 242-243.

L261+263: You give the numbers 34% and 66% and the only reference you give is Fig 7d. I guess I am supposed to be able to derive the 34 and 66 from the numbers of the fits printed on Fig 7d, and here I have two issues: i) the numbers are extremely small and difficult to read and ii) please help the reader how to derive the 34 and 66. These are central numbers from the study and you do not want to leave any doubt about them with the reader.

Ok, done.  $34\% = (19.42 * 100)/56.59$  and  $66\% = (37.1742 * 100)/56.59$ . The numbers came from Fig 7d bottom. See lines 261-264.

L315. Strike "sea the"

Ok, removed.

L336-337: "strong increases ... are limited". Sounds odd. Either "strong increases ... are excluded/absent/etc" or just "increases... are limited".

Ok, done. We opted for the second suggestion such as "increases... are limited". See line 337

Fig 8: In many panels, the legends cover the data, lines and boxes. If you want the reader to see the data, please change this.

Ok, done. See new figure 8.

Sect 3.4: This whole section could use another round on the language. It appears to not have been gone over as thoroughly as the rest of the paper.

Ok, done. Experienced scholarly writer P. C. Taylor who is *native English-speakers* have edited this section in the new version of the manuscript.

L378: "over THE Arctic Ocean"

Ok, done.

L378: "Arctic Ocean", in the figure (Fig 9) you call it "Arctic sea" (which also sounds odd). Please choose one and stick with it.

Ok, Arctic Sea is replaced by Arctic Ocean in the new version of the manuscript. See figure 9

L379: "dampening", in other places you say "damping"

Ok, “dampening” is replaced by “damping” in the new version of the manuscript.

L381: “causes”

Ok, done. See line 382.

L382: “Fig 9gh”: Are panels g and h really the right reference for this sentence?

(Fig. 9ef) is the correct reference. We corrected this in line 383

L393: “consistent”: Consistent with what? With the observed trends? If so, say so.

Yes, consistent with observed trends. This is clearly mentioned in line 394 of the new version of the manuscript.

L404: “sea-ice” In the rest of the paper you write “sea ice”. Choose one.

We choose sea ice in the new version of the manuscript.

L406: “between two consecutive years, the cloud radiative...”.

Ok, done. See line 407.

L422: Why is the Solomon reference written differently from the others?

Ok, we corrected this in line 423 of the current version of the manuscript.

L426: “At the very least,”. I think you are being too modest here. I would suggest something like “On a practical level,”.

Ok, replaced. See line 426.

L434: “with respect”

Ok, done. See line 435.

L436: “RCP8.5” – that is also how you write it in L371.

Ok, done. See line 437.

We thank the reviewer her (his) edits and comments that helped us to improve the manuscript.

# Clouds damp the radiative impacts of Polar sea ice loss

**Authors:** Ramdane Alkama<sup>1\*</sup>, ~~Alessandro Cescatti<sup>4</sup>~~, Patrick C. Taylor<sup>2\*</sup>, Lorea Garcia-San Martin<sup>1</sup>, Herve Douville<sup>3</sup>, Gregory Duveiller<sup>1</sup>, Giovanni Forzieri<sup>1</sup>, ~~and~~ Didier Swingedouw<sup>4</sup> and ~~Alessandro Cescatti<sup>1</sup>~~

Formatted: Not Superscript/Subscript

## Affiliation:

<sup>1</sup> European Commission, Joint Research Centre, Via E. Fermi, 2749, I-21027 Ispra (VA), Italy

<sup>2</sup> NASA Langley Research Center, Hampton, Virginia

<sup>3</sup> Centre National de Recherches Meteorologiques, Meteo-France/CNRS, Toulouse, France

<sup>4</sup> EPOC, Universite Bordeaux 1, Allée Geoffroy Saint-Hilaire, Pessac 33615, France

\*Correspondence to: Ramdane Alkama ([ram.alkama@hotmail.fr](mailto:ram.alkama@hotmail.fr))

~~Patrick C. Taylor ([patrick.c.taylor@nasa.gov](mailto:patrick.c.taylor@nasa.gov))~~

Formatted: Font: TimesNew Roman

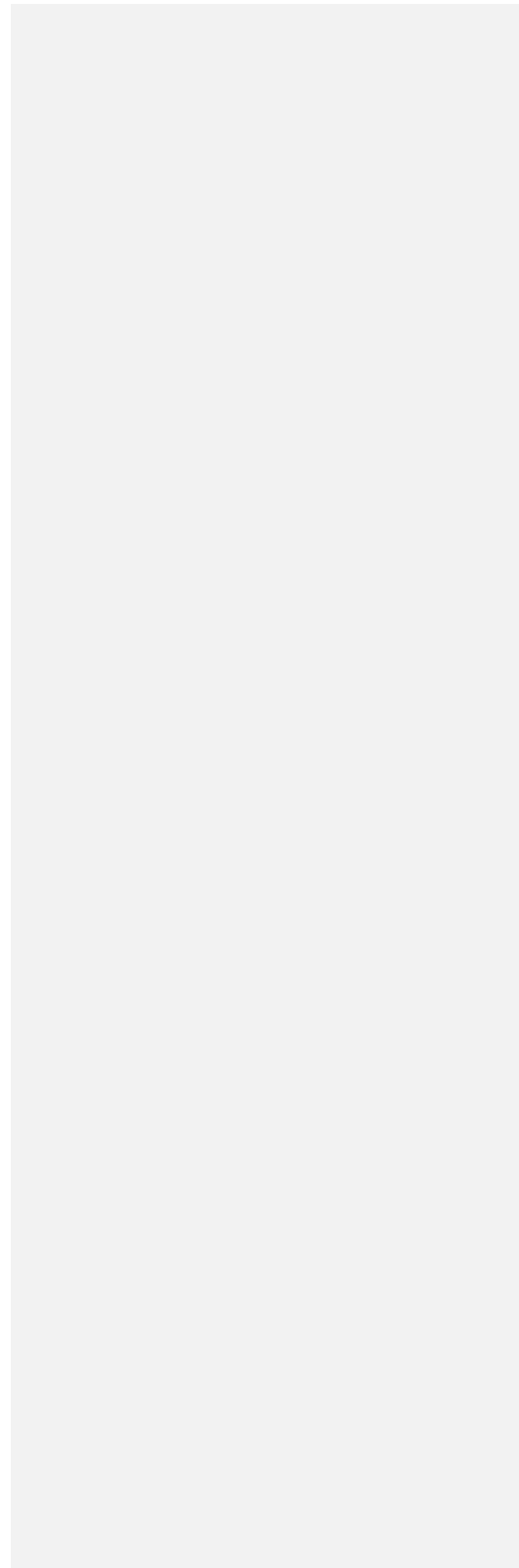
Formatted: Font: (Default)TimesNew Roman, 12 pt

Formatted: Font: TimesNew Roman

## Abstract

Clouds play an important role in the climate system: (1) cooling the Earth by reflecting incoming sunlight to space and (2) warming the Earth by reducing thermal energy loss to space. Cloud radiative effects are especially important in polar regions and have the potential to significantly alter the impact of sea ice decline on the surface radiation budget. Using CERES data and 32 CMIP5 climate models, we quantify the influence of polar clouds on the radiative impact of polar sea ice variability. Our results show that the cloud shortwave cooling effect strongly influences the impact of sea ice variability on the surface radiation budget and does so in a counter-intuitive manner over the polar seas: years with less sea ice and a larger net surface radiative flux show a more negative cloud radiative effect. Our results indicate that  $66 \pm 2\%$  of this change in the net cloud radiative effect is due to the reduction in surface albedo and the remaining  $34 \pm 1\%$  is due to an increase in cloud cover/optical thickness. The overall cloud radiative damping effect is  $56 \pm 2\%$  over the Antarctic and  $47 \pm 3\%$  over the Arctic. Thus, present-day cloud properties significantly reduce the net radiative impact of sea ice loss on the Arctic and Antarctic surface radiation budgets. As a result, climate models must accurately represent present-day polar cloud properties in order to capture the surface radiation budget impact of polar sea ice loss and thus the surface albedo feedback.

36  
37

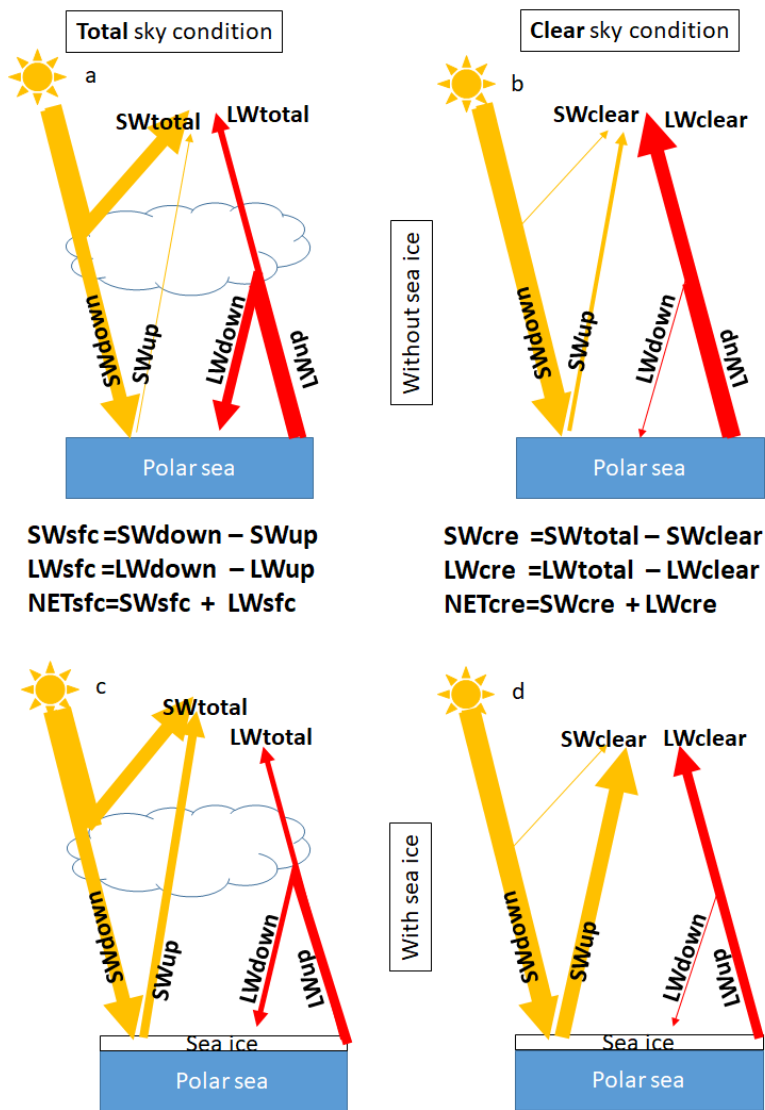


## 38 1. Introduction

39 Solar radiation is the primary energy source for the Earth system and provides the energy driving  
40 motions in the atmosphere and ocean, the energy behind water phase changes, and for the energy  
41 stored in fossil fuels. Only a fraction (Loeb et al., 2018) of the solar energy arriving to the top of  
42 the Earth atmosphere (shortwave radiation, SW) is absorbed at the surface. Some of it is reflected  
43 back to space by clouds and by the surface, while some is absorbed by the atmosphere. In parallel,  
44 the Earth's surface and atmosphere emit thermal energy back to space, called outgoing longwave  
45 (LW) radiation, resulting in a loss of energy (Fig. 1). The balance between these energy exchanges  
46 determines Earth's present and future climate. The change in this balance is particularly important  
47 over the Arctic where summer sea ice is retreating at an accelerated rate (Comiso et al., 2008),  
48 the global albedo is rapidly declining, and surface temperatures are rising at a rate double that of the  
49 global average (Cohen et al., 2014; Graversen et al., 2008), impacting sub-polar ecosystems  
50 (Cheung et al., 2009; Post et al., 2013) and possibly mid-latitude climate (Cohen et al., 2014;  
51 Cohen et al. 2019).

52 Clouds play an important role in modifying the radiative energy flows that determine Earth's  
53 climate. This is done both by increasing the amount of SW reflected back to space and by reducing  
54 the LW energy loss to space relative to clear skies (Fig. 1). These cloud effects on Earth's radiation  
55 budget can be gauged using the Cloud Radiative Effect (CRE), defined as the difference between  
56 the actual atmosphere and the same atmosphere without clouds (Charlock and Ramanathan, 1985).  
57 The different spectral components of this effect can be estimated from satellite observations: the  
58 global average SW cloud radiative effect (SWcre) is negative since clouds reflect incoming solar  
59 radiation back to space resulting in a cooling effect. On the other hand, the LW cloud radiative  
60 effect (LWcre) is positive since clouds reduce the outgoing LW radiation to space generating a  
61 warming effect (Harrison et al., 1990; Loeb et al., 2018; Ramanathan et al., 1989).

62 Cloud properties and their radiative effects exhibits significant uncertainty in the polar regions  
63 (e.g., Curry et al. 1996; Kay and Gettelman 2009; Boeke and Taylor 2016; Kato et al. 2018). For  
64 instance, climate models struggle to accurately simulate cloud cover, optical depth, and cloud  
65 phase (Cesana et al., 2012; Komurcu et al., 2014; Kay et al. 2016). An accurate representation of  
66 polar clouds is necessary because they strongly modulate radiative energy fluxes at the surface, in  
67 the atmosphere, and at the TOA influencing the evolution of the polar climate systems. In addition,  
68 polar cloud properties interact with other properties of the polar climate systems (e.g., sea ice) and  
69 influence how variability in these properties affects the surface energy budget (Qu and Hall 2006;  
70 Kay and L'Ecuyer 2013; Sledd and L'Ecuyer 2019). Moreover, Loeb et al. (2019) documented  
71 severe limitations in the representation of surface albedo variations and their impact on the  
72 observed radiation budget variability in reanalysis products, motivating the evaluation of radiation  
73 budget variability over the polar seas in climate models. In this study, we use the Clouds and the  
74 Earth's Radiant Energy System (CERES) top-of-atmosphere (TOA) and surface (SFC) radiative  
75 flux datasets and 32 Coupled Model Intercomparison Project (CMIP5) climate models to estimate  
76 the relationship between the CRE and the surface radiation budget in polar regions to improve our  
77 understanding of how clouds modulate the surface radiation budget.



78

79

80 **Figure 1** Schematic representation of radiative energy flows in the polar seas under total sky  
 81 conditions (a, c) and clear sky conditions (b, d) for two contrasting surface conditions: without sea  
 82 ice (a, b) and with sea ice (c, d). All fluxes are taken positive downwards.

83

84 **2. Methods and data**

85 **2.1 CERES EBAF Ed4.0 Products:** Surface and TOA radiative flux quantities are taken from the  
86 NASA CERES Energy Balanced and Filled (EBAF) monthly data set (CERES EBAF-TOA\_Ed4.0  
87 and CERES EBAF-SFC\_Ed4.0), providing monthly, global fluxes on a 1°x1° latitude-longitude  
88 grid (Loeb et al., 2018; Kato et al. 2018). CERES surface LW and SW radiative fluxes are used to  
89 investigate the effect of clouds on the surface radiation budget response to sea ice variability over  
90 the polar seas. CERES SFC EBAF radiative fluxes have been evaluated through comparisons with  
91 46 buoys and 36 land sites across the globe, including the available high-quality sites in the Arctic.  
92 Uncertainty estimates for individual surface radiative flux terms in the polar regions range from  
93 12-16 W m<sup>-2</sup> (1σ) at the monthly mean 1°x1° gridded scale (Kato et al. 2018). CERES EBAF-  
94 TOA and SFC radiative fluxes show a much higher reliability than other sources (e.g.,  
95 meteorological reanalysis) and represent a key benchmark for evaluating the Arctic surface  
96 radiation budget (Christensen et al. 2016; Loeb et al. 2019; Duncan et al. 2020).

97 In addition to radiative fluxes, cloud cover fraction (CCF) and cloud optical depth (COD) data  
98 available from CERES EBAF data are used. Monthly mean CCF and COD data are derived from  
99 instantaneous cloud retrievals using the Moderate-resolution Imaging Spectroradiometer  
100 (MODIS) radiances (Trepte et al. 2019). Instantaneous retrievals are then are spatially and  
101 temporally averaged onto the 1°x1° monthly mean grid consistent with CERES EBAF.

102  
103 **2.2 Cloud Radiative Effect:** CRE is used as a metric to assess the radiative impact of clouds on  
104 the climate system, defined as the difference in net irradiance at TOA between total-sky and clear-  
105 sky conditions. Using the CERES Energy Balanced And Filled (EBAF) Ed4.0 (Loeb et al., 2018)  
106 flux measurements and CMIP5 simulated fluxes, CRE is calculated by taking the difference  
107 between clear-sky and total-sky net irradiance flux at the TOA. All fluxes are taken as positive  
108 downwards.

109  $SW_{cre} = SW_{total} - SW_{clear} \quad (1)$

110  $LW_{cre} = LW_{total} - LW_{clear} \quad (2)$

111  $NET_{cre} = SW_{cre} + LW_{cre} \quad (3)$

112  
113 **2.3 Earth's surface radiative budget:** Surface radiative fluxes are taken from the CERES SFC  
114 EBAF Ed4.0 data set (Kato et al., 2018). The net SW and LW fluxes at the surface ( $SW_{sfc}$  and  
115  $LW_{sfc}$ , respectively) are calculated as the difference between the downwelling  $SW_{down}$  ( $LW_{down}$ )  
116 and upwelling  $SW_{up}$  ( $LW_{up}$ ) as shown in equations 4 (5).

117  $SW_{sfc} = SW_{down} - SW_{up} \quad (4)$

118  $LW_{sfc} = LW_{down} - LW_{up} \quad (5)$

119  $NET_{sfc} = SW_{sfc} + LW_{sfc}$  (6)

120 **2.4 Sea ice concentration:** Sea ice concentration (SIC) data are from the National Snow and Ice  
 121 Data Center (NSIDC, <http://nsidc.org/data/G02202>). This data set is a Climate Data Record (CDR)  
 122 of SIC from passive microwave data and provides a consistent, daily and monthly time series of  
 123 SIC from 09 July 1987 through the most recent processing for both the North and South Polar  
 124 regions (Peng et al., 2013; W. Meier, F. Fetterer, M. Savoie, S. Mallory, R. Duerr, 2017). The data  
 125 is provided on a 25 km x 25 km grid. We used the latest version (Version 3) of the SIC CDR  
 126 created with a new version of the input product, from Nimbus-7 SMMR and DMSP SSM/I-SSMIS  
 127 Passive Microwave Data.

128 **2.5 Polar seas:** We define the polar seas as ocean regions where the monthly SIC is larger than  
 129 10% at least one month during 2001-2016 period. Polar seas extent is shown in Figure S1.

130 **2.6 CMIP5 Models** To reconstruct the historical CRE and surface energy budget and project their  
 131 future changes, we used an ensemble of simulations conducted with 32 climate models (models  
 132 used are shown in Figure 3 and S3) contributing to the Coupled Model Intercomparison Project  
 133 Phase 5 (CMIP5) (Taylor et al., 2012). These model experiments provided: historical runs (1850-  
 134 2005) in which all external forcings are consistent with observations and future runs (2006-2100)  
 135 using the RCP8.5 emission scenarios (Taylor et al., 2012). The comparison with the satellite data  
 136 is made over 2001-2016 by merging historical runs 2001-2005 with RCP8.5 2006-2016.

137 **2.7 Estimation of the local variations in radiative flux, cloud cover, and cloud optical depth**  
 138 **concurrent with changes in sea ice concentration**

139 This study employs a novel method for quantifying the variations in radiative fluxes and cloud  
 140 properties with SIC. This methodology leverages inter-annual variability of sea ice cover to assess  
 141 these relationships. Figure 2 schematically shows the methodology based on the following steps.  
 142 We use  $SW$  as an example and apply the approach in the same way to other variables.

143 1)  $\Delta SW_j$  values are summarized in a schematized plot (Figure 2a) where each cell  $j$  in such plot  
 144 shows the average  $\Delta SW_m$  observed for all possible combinations of SIC at a grid box between two  
 145 consecutive observation years (year  $y_i$  and  $y_i+1$  from time period 2001-2016) displayed on the X  
 146 and Y axes, respectively. For the sake of clarity in Figure 2 the X and Y axes report SIC in intervals  
 147 of 10%, while in Figure 5, 6, 7, S5 and S6 the axes are discretized with 2% bins.

148 2) Because of the regular latitude/longitude grid used in the analysis, the area of the grid cells ( $a_m$ )  
 149 varies with the latitude. The energy signal ( $\Delta SW_j$ ) is therefore computed as an area weighted  
 150 average (Equation 7) where M is the number of grid cells that are used to compute cell  $j$  in the  
 151 schematised plot Fig 2a. Figure 2b shows the total area of all these grid cells as described by  
 152 Equation 8.

153 
$$\Delta SW_j = \frac{\sum_{m=1}^M a_m \Delta SW_m}{\sum_{m=1}^M a_m}$$
 (7)

Field CodeChanged



154  $A_j = \sum_{m=1}^M a_m$  (8)

155

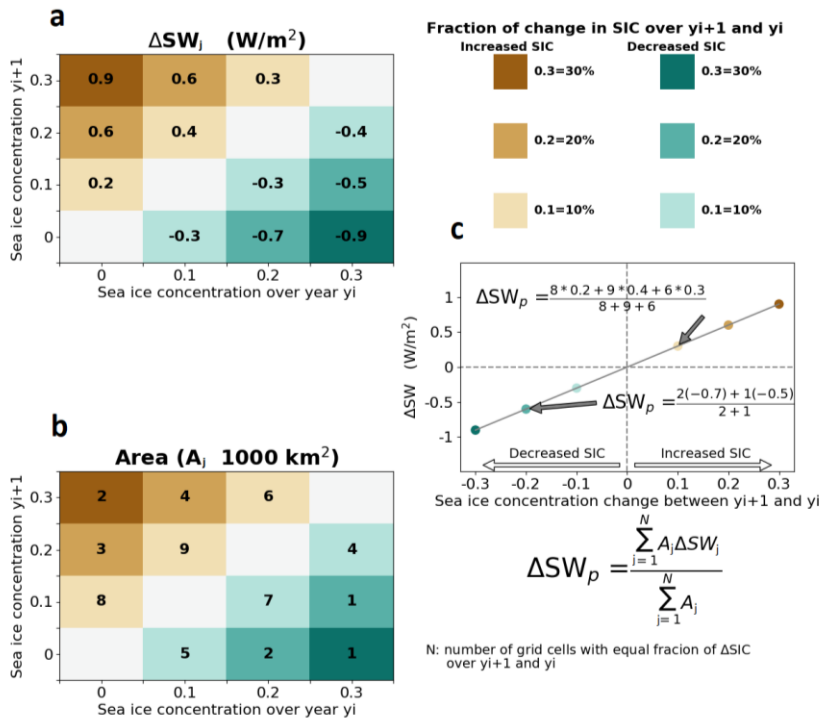
156 3) Calculation of the area weighted average ( $\Delta SW_p$ ) of the energy signal of all  $N$  cells with the  
 157 same fraction  $X$  of a change in SIC (shown with the same colour in Figure 2a) Equation 9.

158 
$$\Delta SW_p = \frac{\sum_{j=1}^N A_j \Delta SW_j}{\sum_{j=1}^N A_j}$$
 (9)

159  $\sum_{j=1}^N A_j$  is the total area of all grid cells with a particular SIC change.

160  $\Delta SW_p$  is the energy weighted average of all grid cells with a particular SIC change.

161



162

163 **Figure 2** Schematic representation of the methodology used to quantify the energy flux sensitivity  
 164 to changes in sea ice concentration as a linear regression between the percentage of sea ice  
 165 concentration and the variation in energy flux (right panel) using SW energy flux data and sea ice  
 166 concentration defined in the left panels.

167

168 The average energy signals ( $\Delta SW_p$ ) per class of sea ice concentration change are reported in a  
169 scatterplot (Fig. 2 right panel) and used to estimate a regression line with zero intercept.

170 The slope  $S$  of this linear regression represents the local SW energy signal generated by the  
171 complete sea ice melting of a  $1^\circ$  grid cell. The weighted root mean square error (WRMSE) of the  
172 slope is estimated by Equation 10, where  $p$  represents one of the  $NP$  points in the scatterplot (Fig.  
173 2 right panel) and  $X_p$  is the relative change in sea ice concentration in the range  $\pm 1$  (equivalent to  
174  $\pm 100\%$  of sea ice cover change).

$$175 \quad WRMSE = \sqrt{\frac{\sum_{p=1}^{NP} A_p (\Delta SW_p - S X_p)^2}{\sum_{p=1}^{NP} A_p}}, \quad \text{where } A_p = \sum_{j=1}^N A_j \quad (10)$$

## 176 2.8 Diagnosis of contributions to SWcre

177 SWcre at the surface for the year  $y_i$  (Eq. 11) and year  $y_{i+1}$  (Eq. 12) is function of surface albedo  
178  $\alpha$ , SWdown under clear sky conditions ( $SW \downarrow_{ctr}$ ) and SWdown under total sky conditions  
179 ( $SW \downarrow_{tot}$ ).

$$180 \quad SWcre_{y_i} = (1 - \alpha_{y_i})(SW \downarrow_{tot,y_i} - SW \downarrow_{ctr,y_i}) \quad (11)$$

$$181 \quad SWcre_{y_{i+1}} = (1 - \alpha_{y_{i+1}})(SW \downarrow_{tot,y_{i+1}} - SW \downarrow_{ctr,y_{i+1}}) \quad (12)$$

182

183 Using the first-order Taylor series expansion to (11) yields

$$184 \quad \Delta SWcre_{y_{i+1}-y_i} \cong$$
$$185 \quad (-\Delta \alpha_{y_{i+1}-y_i})(SW \downarrow_{tot,y_i} - SW \downarrow_{ctr,y_i}) + (1 - \alpha_{y_i})\Delta_{y_{i+1}-y_i}(SW \downarrow_{tot} - SW \downarrow_{ctr}) \quad (13)$$

186

187 Where

$$188 \quad \Delta_{y_{i+1}-y_i}(SW \downarrow_{tot} - SW \downarrow_{ctr}) \cong (SW \downarrow_{tot,y_{i+1}} - SW \downarrow_{ctr,y_{i+1}}) - (SW \downarrow_{tot,y_i} - SW \downarrow_{ctr,y_i}) \quad (14)$$

189

190 Separating the terms yields,

$$191 \quad \Delta SWcre_{AlbLB} \cong (-\Delta \alpha_{y_{i+1}-y_i})(SW \downarrow_{tot,y_i} - SW \downarrow_{ctr,y_i}) \quad (15)$$

192 Where  $\Delta SWcre_{AlbLB}$  is the part of SWcre change that is induced by the change in surface albedo.

193

$$194 \quad \Delta SWcre_{cloud} \cong (1 - \alpha_{y_i})\Delta_{y_{i+1}-y_i}(SW \downarrow_{tot} - SW \downarrow_{ctr}) \quad (16)$$

195 Where  $\Delta SWcre_{cloud}$  is the part of SWcre change that is induced by the change in cloud cover and cloud  
196 optical depth.

197  $\Delta SWcre_{y_{i+1}-y_i} \cong \Delta SWcre_{AlbLB} + \Delta SWcre_{cloud}$  (17).

198 The above equations are used in figure 7 and S5.

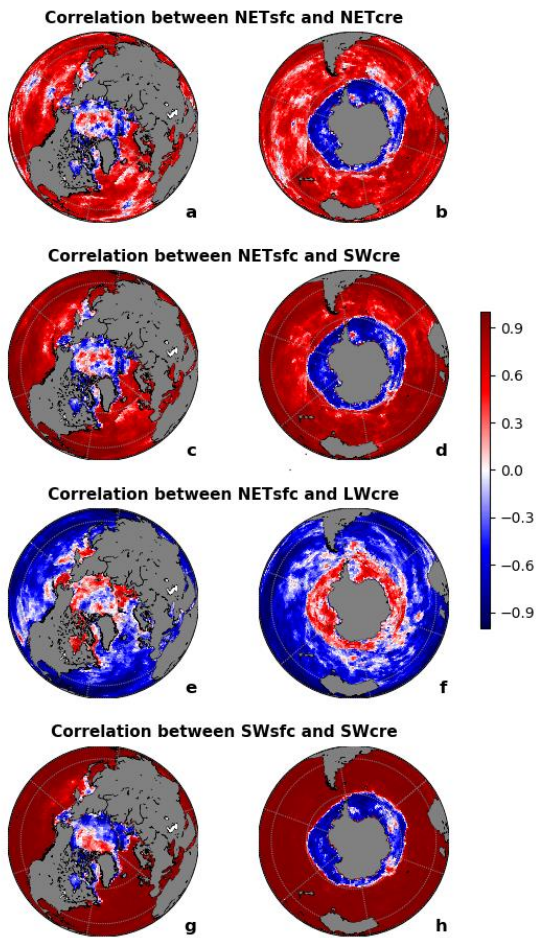
199

### 200 3. Results and discussions

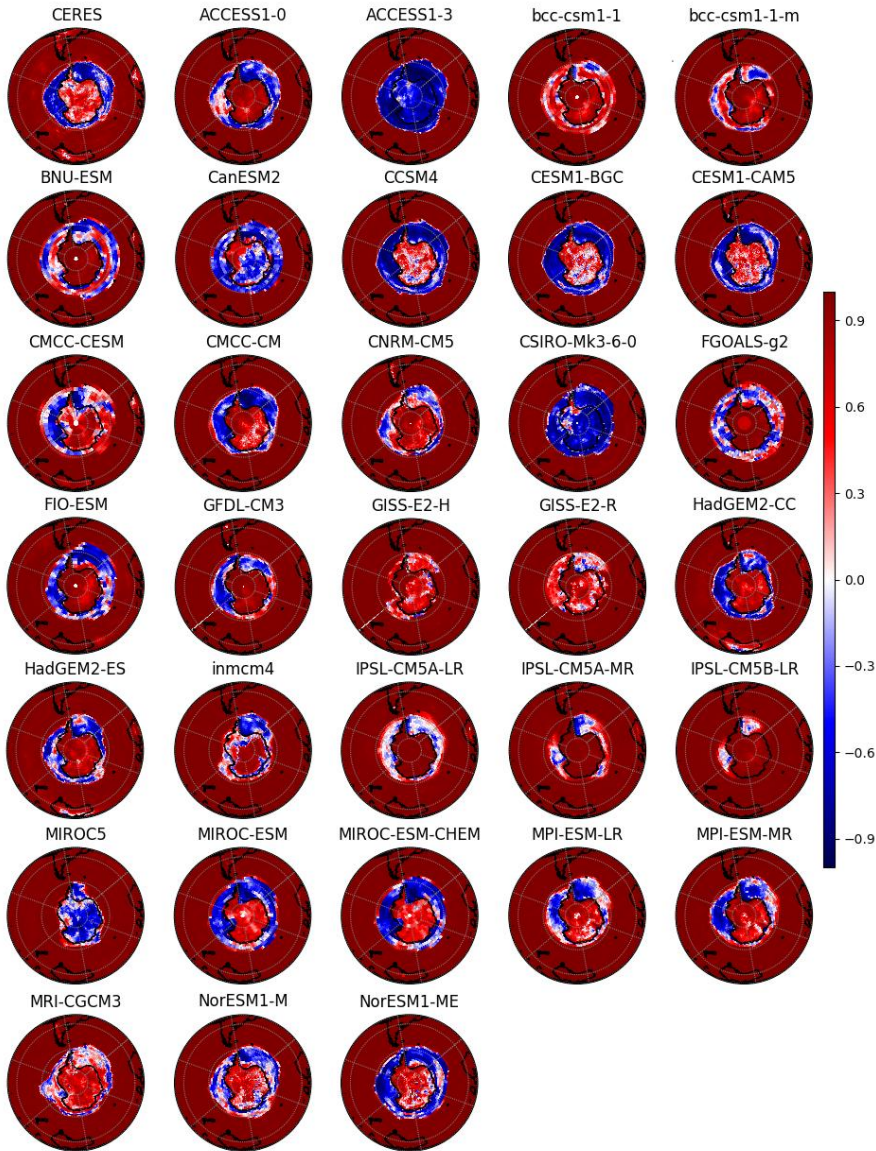
#### 201 3.1 Negative correlation patterns between cloud radiative effect and surface radiation on 202 polar seas

203

204 Given the known cloud influence on the surface radiative budget, a positive correlation between  
205 TOA CRE and surface radiative budget is expected (the amount of absorbed radiation at the surface  
206 decreases with a more negative SWcre and a less positive LWcre). Figure 3 illustrates a positive  
207 correlation between the annual mean NETcre and NETsfc over much of the global ocean using the  
208 CERES TOA flux data from 2001-2016. However, our analysis reveals the opposite pattern over  
209 the polar seas (defined in section 2.5) where the correlation is negative over the Antarctic and  
210 partly negative over the Arctic (Bering Strait, Hudson Bay, Barents Sea and the Canadian  
211 Archipelago; Fig. 3ab). Considering the SWcre and LWcre components, we find that the SWcre  
212 (Fig. 3cd) shows a similar pattern of correlation as the NETcre (Fig. 3ab) but with a stronger  
213 magnitude, while LWcre generally shows the opposite correlations (Fig. 3ef). This suggests that  
214 the factors influencing SWcre are responsible for the sharp contrast in the correlation found in the  
215 polar regions. Indeed, SWsfc and SWcre (Fig. 3gh) show the sharpest and most significant contrast  
216 between the polar regions and the rest of the world (Fig. S2 is similar to Fig. 3 but only significant  
217 correlations at the 95% confidence level are reported in blue and red colors). Overall, climate  
218 models are able to reproduce the spatial pattern of the observed SW correlation, but also show a  
219 large inter-model spread in the spatial extent of the phenomena (Fig. 4 and S3). On the other hand,  
220 several models completely fail to reproduce the correlation. ACCESSI-3, MIROC5, CanESM2  
221 and CSIRO-Mk3-6-0 models show negative correlation over Antarctic continent in contrast to  
222 observed positive correlation. Some models, like IPSL-CM5B-LR, GISS-E2-R and bcc-csm1-1,  
223 fail to reproduce the observed negative correlation over the Southern Ocean. This suggests that  
224 these models contain misrepresentations of the relationships SWcre and NETsfc likely resulting  
225 from errors in the relationships between sea ice, surface albedo, cloud cover/thickness, and their  
226 influence on surface radiative fluxes that could severely impact their projections. Moreover, Fig.  
227 4 demonstrates that simple correlations between NETsfc and the individual radiation budget terms  
228 represents a powerful metric for climate model evaluation allows for a quick check for realistic  
229 surface radiation budget variability in polar regions.



230  
 231 **Figure 3** Correlation between TOA CRE and surface radiation budget terms over 2001-2016 from  
 232 CERES measurements for the Northern Hemisphere (aceg) and Southern Hemisphere (bdfh) polar  
 233 sea. Positive correlations shown by the red color indicate that years with less NET sfc coincide  
 234 with years where NET cre has a stronger cooling effect and *vice versa*.



235  
 236 **Figure 4** Correlation between SWcre and SWsfc shown by 32 CMIP5 earth system models and  
 237 CERES between 2001 and 2016 over the Southern Hemisphere.

238

### 239 3.2 Effects of sea ice concentration change

240 We illustrate that the apparent contradiction over the polar seas between NET<sub>cre</sub> and NET<sub>sfc</sub>  
241 found in Fig 3ab is caused by the factors contributing to the SW fluxes. This can be explained by:  
242 (I) SW<sub>cre</sub> can change even if cloud properties are held constant due to the changes in clear-sky  
243 radiation induced by changes in sea ice and surface albedo. When surface albedo is reduced, the  
244 surface absorbs more sunlight at the surface resulting in a greater SW<sub>total</sub>. At the same time,  
245 SW<sub>clear</sub> increases since the lower albedo allows a larger fraction of the extra downwelling SW at  
246 the surface to be absorbed (see Fig. 1). Therefore, SW<sub>cre</sub> becomes more negative even in the  
247 absence of cloud changes (a purely surface-related effect); (II) On the other hand, the relationship  
248 between cloud cover/thickness and sea ice could lead to cloudier Polar seas under melting sea ice  
249 (Abe et al., 2016; Liu et al., 2012) such that the SW<sub>cre</sub> decreases (increasing the amount of SW  
250 reflected back to space by clouds, see Fig. 1), thus the cloud cooling effect is enhanced  
251 concurrently with melting sea ice (a purely cloud-related effect). Both of these factors occur  
252 simultaneously.

253  
254  
255 Over the Antarctic Ocean seas, analysis of the year-to-year changes in SW<sub>down</sub> stratified in 2%  
256 SIC bins retrieved from satellite microwave radiometer measurements (see section 2.7) shows an  
257 increase in SW<sub>down</sub> with increased SIC and *vice-versa* (Fig. 5a). This suggests that years with  
258 higher SIC also have fewer and/or thinner clouds (Liu et al., 2012) (Fig. 6), larger SW<sub>down</sub> and  
259 also larger upward SW radiation (SW<sub>up</sub>) (Fig. 5b), due to higher surface albedo (Fig. S4).  
260 Consequently, these years show a more negative SW<sub>sfc</sub> (Fig. 5c) and thus are characterized by  
261 stronger surface cooling. Furthermore, fewer clouds implies a reduction of the cloud cooling effect  
262 (less negative SW<sub>cre</sub>) as described above in process (II), this accounts for  $(19.42 * 100)/56.59 =$   
263  $34 \pm 1\%$  (Fig. 7d bottom) of the total change in SW<sub>cre</sub>, and as described in process (I) the increase  
264 in the surface albedo also makes SW<sub>cre</sub> less negative and explains  $(37.17 * 100)/56.59 = 66 \pm$   
265  $2\%$  of the observed change (Fig. 7d bottom). Thus, the observed negative correlation between  
266 SW<sub>cre</sub> and SW<sub>sfc</sub> over the polar seas results from the larger effects of process (I) than (II). Similar  
267 results are found over the Arctic Ocean with slightly different sensitivity (Fig. S5, S6). This  
268 difference is tied to differences in sun angle/available sunlight, as Antarctic sea ice is concentrated  
269 at lower latitudes than Arctic sea ice.

270  
271 Using the regression relationships derived from our composite analysis, we estimate the magnitude  
272 of the cloud effect. For the Antarctic system, we use the numbers found in Figure 5e where we  
273 find the annual mean relationship between NET<sub>sfc</sub> (in W/m<sup>2</sup>) and SIC (fraction between 0 and 1),  
274 and NET<sub>cre</sub> (in W/m<sup>2</sup>) and SIC (fraction between 0 and 1).

$$275 \Delta \text{NET}_{\text{sfc}} = (-36.61 \pm 0.72) \Delta \text{SIC} \quad (18)$$

$$276 \Delta \text{NET}_{\text{cre}} = (47.03 \pm 1.01) \Delta \text{SIC} \quad (19)$$

277  
278 When excluding the CRE, the  $\Delta \text{NET}_{\text{sfc}}$  would be equal to  $(-36.61 - 47.03) \Delta \text{SIC} = -83.64 \Delta \text{SIC}$ .

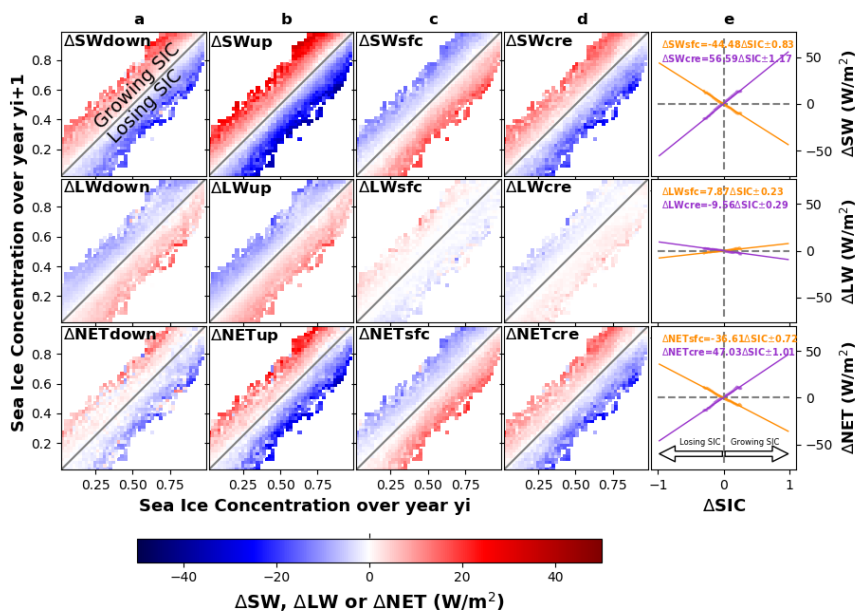
279 We estimate that the existence of clouds and their property variations are damping the potential



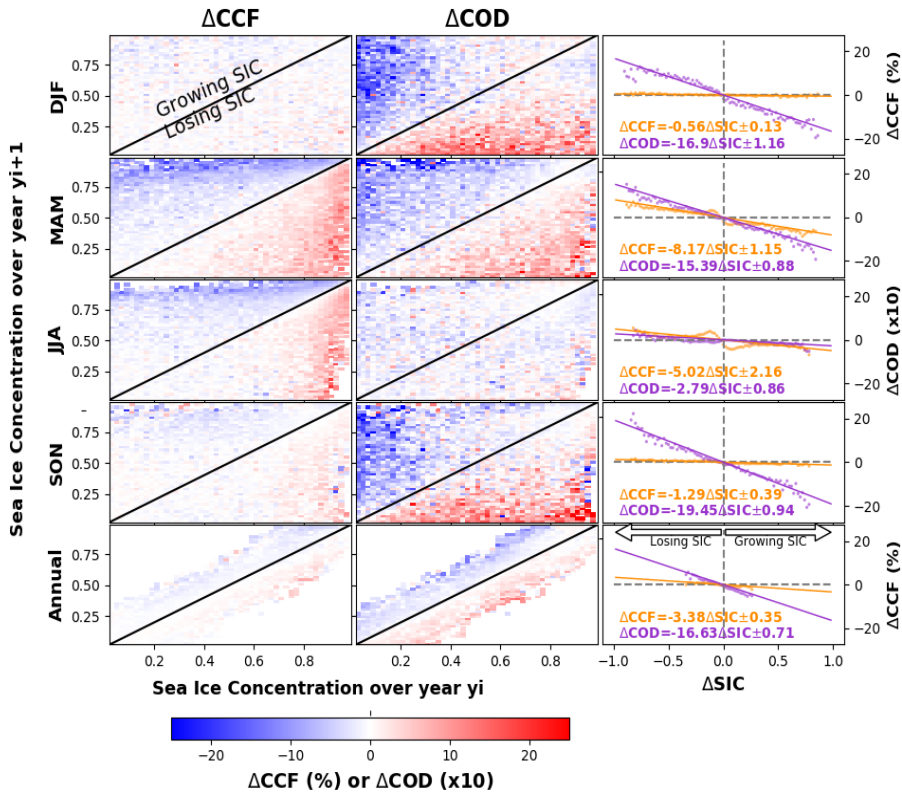
280 increase in the NETsfc within the Antarctic system due to the surface albedo decrease from sea ice  
 281 melt by 56% (47.03/83.64). The uncertainty is calculated by summing the uncertainties shown in  
 282 equation (18) and (19) as follows:  $(0.72^2+1.01^2)^{1/2}/83.64=2\%$ .

283 Similarly, over the Arctic (Fig. S5), we compute the cloud influence on the surface net radiative  
 284 budget that covaries with sea ice loss is  $47\pm 3\%$ , in agreement with the study of Sledd and L'Ecuyer  
 285 (2019).

286

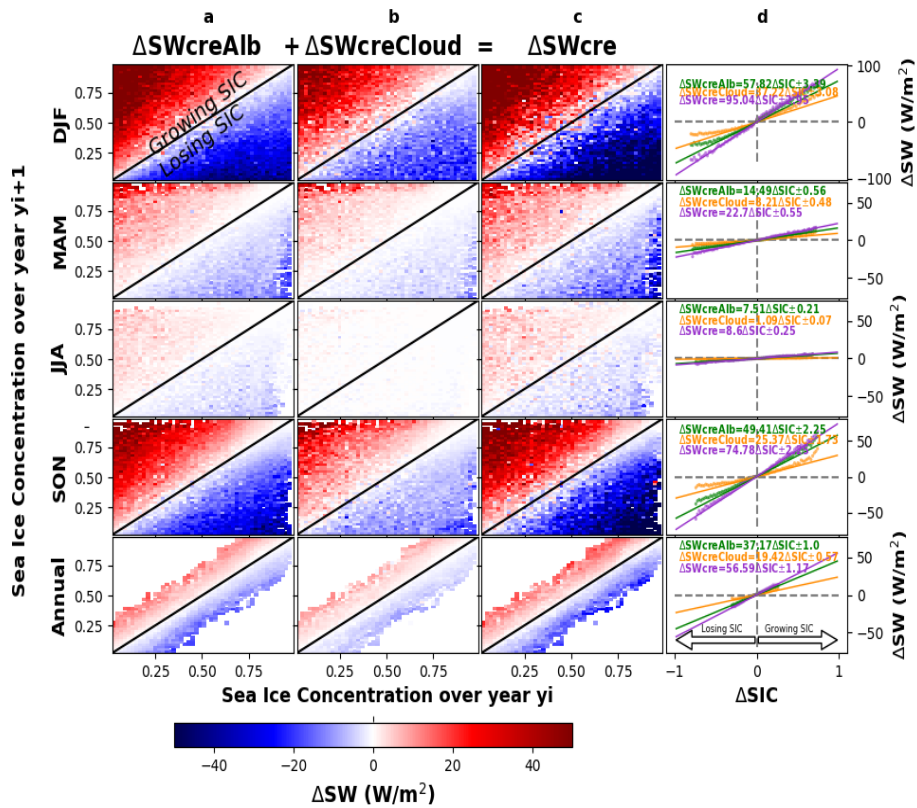


287 **Figure 5** Annual changes in SW, LW and NET as function of SIC. Annual changes in SW (top),  
 288 LW (middle) and NET (bottom) of radiative down (a), up (b), sfc=down-up (c) and cre (d) over  
 289 Antarctic Oceansa as function of SIC change between two consecutive years  $y_{i+1}$  and  $y_i$  from  
 290 2001-2016 time period. The top triangles in (c top) refers to the increase (growing) in SIC while  
 291 the blue color means a reduction (cooling) in SWsfc. Whereas, the top triangles in (d) refers to the  
 292 increase in SIC while the red color means an increase (decreasing the cooling role of clouds) in  
 293 SWcre. Each dot in column (e) represents the average of one parallel to the diagonal in (c) or (d)  
 294 as described in the Section 2.7.  
 295  
 296



297  
 298 **Figure 6** Seasonal and annual changes in cloud cover fraction (CCF) and cloud optical depth  
 299 (COD) over the Antarctic polar sea region as a function of SIC change between two consecutive  
 300 years  $y_{i+1}$  and  $y_i$  from 2001-2016 time period. In order to use the same scale, COD has been  
 301 multiplied by a factor 10. The top triangles in the two first columns refer to the increase (growing)  
 302 in SIC while the blue color means a reduction in CCF or COD.  
 303





304  
 305 **Figure 7** Seasonal and annual changes in  $SW_{creAlb}$ ,  $SW_{creCloud}$  and  $SW_{cre}$  over the Antarctic  
 306 polar sea region as function of SIC change between two consecutive years  $y_{i+1}$  and  $y_i$  from 2001-  
 307 2016 time period. The analysis is based on method described in section 2.7 and observations from  
 308 satellites data.

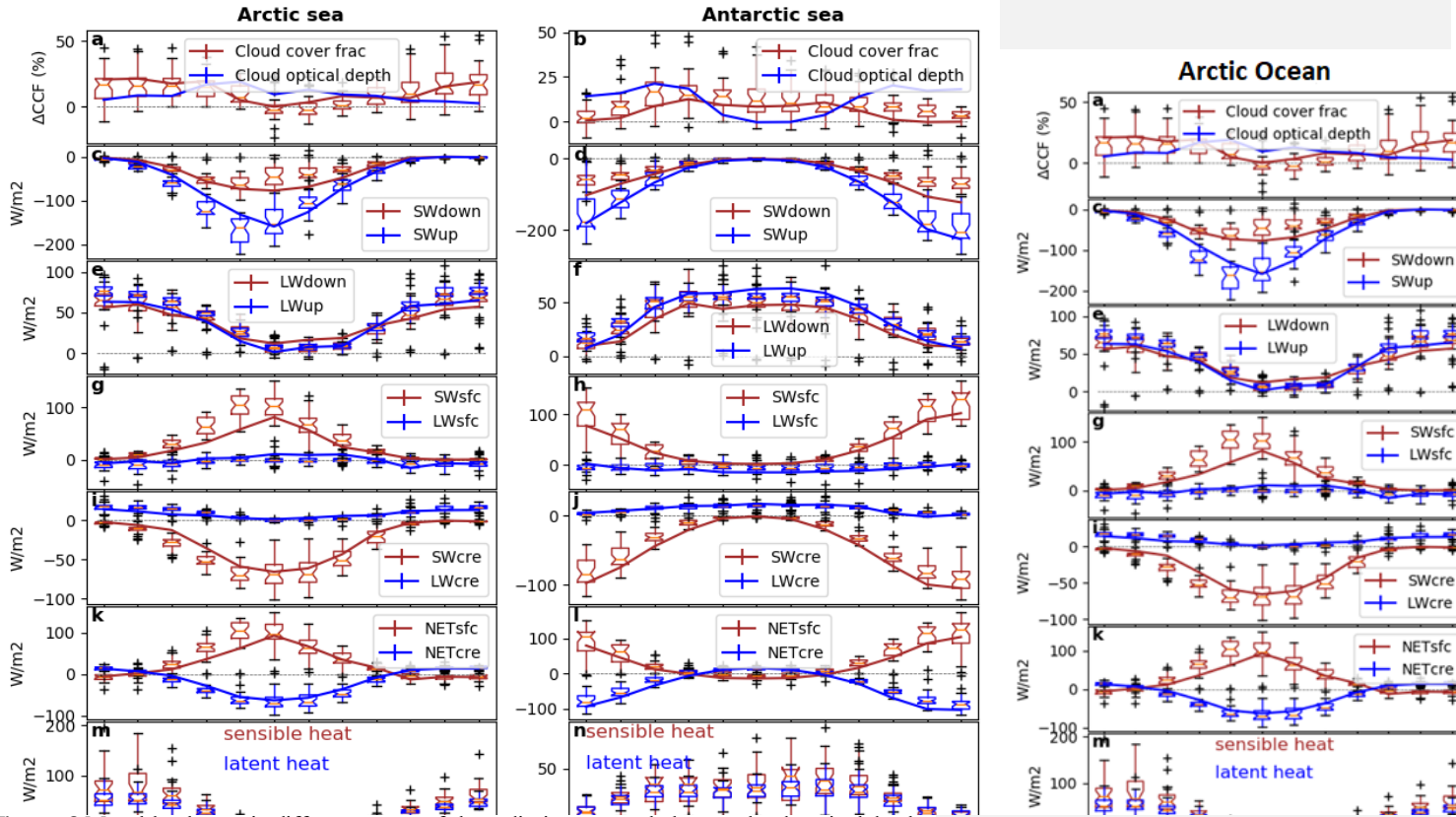
309  
 310  
 311  
 312  
 313  
 314  
 315

316 Altogether the results suggest clouds substantially reduce the impact of sea ice loss on the surface  
317 radiation budget and thus the observed ~~sea-ice~~ sea ice albedo feedback. This effect in the polar  
318 climate system leads to a substantial reduction ( $56\pm 2\%$  over the Antarctic and  $47\pm 3\%$  over the  
319 Arctic) of the potential increase in NET sfc in response to sea ice loss. This magnitude is similar to  
320 a previous study (Qu and Hall 2006) showing across a climate model ensemble that clouds damped  
321 the TOA effect of land surface albedo variations by half. Sledd and L'Ecuyer (2019) also  
322 determined that the cloud damping effect (also referred to as cloud masking) of the TOA albedo  
323 variability results from Arctic sea ice changes was approximately half. Despite this mechanism,  
324 the sharp reduction in Arctic surface albedo has dominated the recent change in the surface  
325 radiative budget and has led to a significant increase in NET sfc since 2001 in the CERES data  
326 (Duncan et al. 2020). These results demonstrate that the trends in polar surface radiative fluxes are  
327 driven by reductions in SIC and surface albedo and that clouds have partly mitigated the trend (i.e.,  
328 a damping effect). Our findings highlight the importance of processes that control sea ice albedo  
329 (i.e. sea ice dynamics, snowfall, melt pond formation, and the deposition of black carbon), as the  
330 surface albedo of the polar seas in regions of seasonal sea ice is crucial for the climate dynamics.

### 331 3.3 Sensitivity of the surface energy budget to variability of sea ice concentration

332 Our results are consistent with other recent studies (Taylor et al., 2015; Morrison et al. 2018) that  
333 demonstrate a CCF response to reduced sea ice in fall/winter but not in summer (Figure 8a) over  
334 the Arctic ~~Ocean~~. The lack of a summer cloud response to sea ice loss is explained by the  
335 prevailing air-sea temperature gradient, where near surface air temperatures are frequently warmer  
336 than the surface temperature (Kay and Gettelman 2009). Surface temperatures in regions of sea  
337 ice melt hover near freezing due to the phase change, whereas the atmospheric temperatures are  
338 not constrained by the freezing/melting point. Despite reduced sea ice cover, ~~strong~~ increases in  
339 surface evaporation (latent heat) are limited (Fig. 8mn), as also suggested by the small trends in  
340 surface evaporation rate derived from satellite-based estimates (Boisvert and Stroeve, 2015; Taylor  
341 et al., 2018). We argue that the strong increase of SWcreCloud under decreased sea ice observed  
342 during summer is induced by larger values of COD (Fig. 8a), which depend on the liquid or ice  
343 water content. We also show that the relationships derived from our observation-driven analysis  
344 match the projected changes in the Arctic and Antarctic surface energy budget in the median  
345 CMIP5 model ensemble (Fig. 8). However, we find a large spread amongst climate models that  
346 indicates considerable uncertainty.

347 Analyzing the seasonal cycle of the sensitivity of the surface energy budget to SIC variability, we  
348 found that SWsfc (SWcre) explains most of the observed changes in the NET sfc (NETcre) during  
349 summer, while LWSfc plays a minor role (Fig. 8). In contrast, during winter LWSfc (LWcre)  
350 explains most of the observed changes in the NET sfc (NETcre). In general, the median of the 32  
351 CMIP5 (Taylor et al., 2012) climate models captures the observed sensitivity of the radiative  
352 energy budget and cloud cover change to SIC but the spread between climate models is large,  
353 especially for CCF. We have to note here that, the numbers reported in Figure 8 are for 100% SIC  
354 loss, while the ones reported in the previous figures (Fig. 5, 6 and 7) are for 100% SIC gain,  
355 explaining the opposite sign.  
356



359 **Figure 8** Monthly change in different terms of the radiative energy balance, cloud optical depth  
 360 (COD) and cloud cover fraction (CCF) extrapolated from observations for a hypothetical 100%  
 361 decrease in SIC over the areas where SIC change was observed during the period 2001-2016. This  
 362 estimate came from the use of a linear interpolation of the change of different parts of the energy  
 363 budget, COD and CCF as function of a change in SIC coming from all possible combinations of  
 364 couplets of consecutive years for a given month from 2001 to 2016 and for all grid cells for which  
 365 SIC is larger than zero in one of the two years (see section 2.7). CERES data are shown by solid  
 366 lines (the standard deviation of the slopes are also reported but are too small to be visible) while  
 367 CMIP5 models are shown by boxplot and the box (are in same color as observations) represents  
 368 the first and third quartiles (whiskers indicate the 99% confidence interval and black markers show  
 369 outliers). In order to use the same scale, COD has been multiplied by a factor 10.

372 **3.4 Projections and uncertainties of cloud radiative effects on surface energy budget**

373 Under the RCP8.5 scenario (~~a “business as usual ease”~~; Taylor et al., 2012), CMIP5 models show  
374 an increase in SWsfc over the Arctic ~~Ocean Ocean~~ (Fig. 9a), consistent with the expected ~~large~~  
375 decrease in the SIC (Comiso et al., 2008; Serreze et al., 2007; Stroeve et al., 2007). This increase  
376 in SWsfc occurs despite the ~~relatively~~ large, concurrent and opposing change in ~~cloud cooling~~  
377 ~~effect~~ (SWcre). ~~Projections of Future-LW flux changeses~~ (Fig. 9c) ~~are expected to will likely~~ play  
378 a ~~smaller~~ but non-negligible role on total energy budget ~~in summer~~ by ~~slightly further~~ increasing  
379 NET sfc (Fig. 9e) ~~and reducing NETcre~~. In addition, CMIP5 models ~~show clearly indicate~~ that by  
380 2100, the magnitude of the ~~decrease in~~ NETcre ~~decrease will be is~~ slightly smaller than the  
381 increase in NET sfc (Fig. 9e) over ~~the Arctic Ocean~~; ~~while~~ the Antarctic polar sea region  
382 shows the opposite (Fig. 9f). This is in line with the estimated dampening effect of clouds coming  
383 from CERES over 2001-2016 that is about 47±3% in the Arctic and 56±2% in the Antarctic.  
384 ~~Indeed, the~~ stronger cloud damping effect in the Antarctic region ~~causes is indicated by the~~  
385 ~~stronger negative change in the~~ NETcre ~~to become even more negative in the Antarctic compared~~  
386 ~~than to~~ the Arctic (Fig. 9efg).

387  
388 Large uncertainties remain in the ~~rate of decline rate of~~ summer sea ice ~~decline~~ and the timing of  
389 the first ~~occurrence of a~~ sea ice-free Arctic summer (Arzel et al., 2006; Zhang and Walsh, 2006).  
390 ~~The reason processes responsible for behind~~ the large ~~inter-model~~ spread between climate models  
391 ~~is are still under debated scrutiny~~ (Holland et al., 2017; Simmonds, 2015; Turner et al., 2013).  
392 ~~However, recent studies reaffirm the important role of the sea ice albedo feedback and the~~  
393 ~~associated increased upper Arctic Ocean heat content~~ (Holland and Lundrum 2015; Boeke and  
394 Taylor 2018) as well as the contributions from temperature-related feedbacks (Pithan and  
395 Maruitsen 2014; Stuecker et al. 2018). ~~In this study Figure 9gh, we explored the shows that the~~  
396 annual mean Arctic and Antarctic sea ice extent trend from 32 CMIP5 models ~~and possesses a~~  
397 ~~find a~~ large positive correlation with the simulated trend in the SWdown, ~~in line with previous~~  
398 ~~studies~~ (Holland and Lundrum 2015) (Figure 9gh). ~~We note that from the 32 CMIP5 models tested,~~  
399 ~~only a few show SWdown trends consistent with observed trends in SWdown and SIC over 2001-~~  
400 ~~2016~~ (Figure 9gh). ~~Understanding the factors responsible for this disagreement between model-~~  
401 ~~simulated and observed trends in SWdown and SIC may be provide insights into the processes~~  
402 ~~responsible for the inter-model spread in Arctic climate change projections and are the subject of~~  
403 ~~future work. This We also find analysis suggests~~ that the models ~~showing with~~ a larger trend in  
404 cloud cover also ~~show possess a~~ larger decreases in sea ice extent, ~~and suggesting that~~ a stronger  
405 coupling ~~between~~ of these two variables that may ~~become stronger occur~~ in the future. However,  
406 the direction of causality between the two variables is unclear ~~and also requires further study.~~ ~~We~~  
407 ~~also note that from the 32 models tested, only few show consistent with the observed trends in~~  
408 ~~both SWdown and SIC over 2001-2016~~ (Figure 9gh).

409

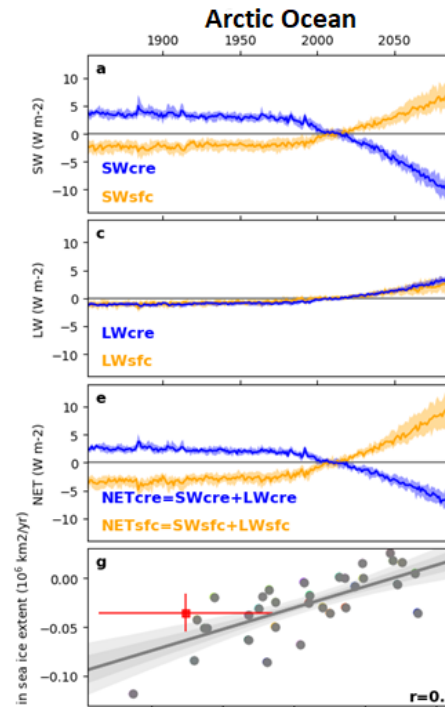
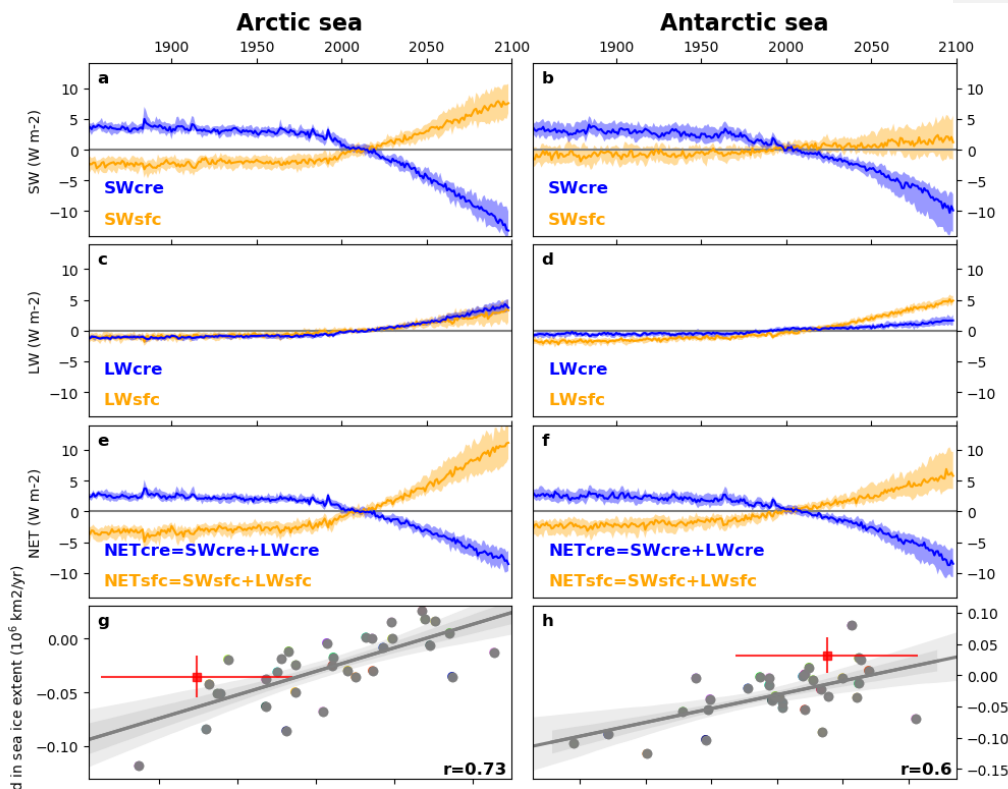
410 **4. Conclusion**

411 The manuscript addresses two important climate science topics, namely the role of clouds and the  
412 fate of polar sea ice. The work is grounded in a long time series of robust satellite observations  
413 that allowed us to document an important damping effect in the polar cloud-sea ice system using  
414 a unique inter-annual approach. Our results agree with several previous works that approached the  
415 problem from a different perspective (Hartmann and Ceppi 2014; Sledd and L'Ecuyer 2019). In  
416 addition, we show how 32 state-of-the-art climate models represent aspects of the surface radiation  
417 budget over the polar seas.

418  
419 Our data-driven analysis shows that polar sea ice and clouds interplay in a way that substantially  
420 reduces the impact of the sea ice loss on the surface radiation budget. We found that when sea ice  
421 cover is reduced between two consecutive years, ~~that~~ the cloud radiative effect becomes more  
422 negative, damping the total change in the net surface energy budget. The magnitude of this effect  
423 is important. Satellite data indicates that the more negative cloud radiative effect reduces the  
424 potential increase of net radiation at the surface by approximately half. One-third of this cloud  
425 radiative effect change is induced by the direct change in cloud cover/thickness, while two-thirds  
426 of this change results from the surface albedo change.

427  
428 In addition, we demonstrated that the models that show larger trends in polar sea ice extent also  
429 show larger trends in surface net solar radiation. In order to understand current and future climate  
430 trajectories, model developments should aim at reducing uncertainties in the representation of  
431 polar cloud processes in order to improve the simulation of present-day cloud properties over the  
432 polar seas. Present-day Arctic and Antarctic cloud properties strongly influence the model  
433 simulated cloud damping effect on the radiative impacts of sea ice loss.

434  
435 Future cloud changes and sea ice evolution represent major uncertainties in climate projections  
436 due to the multiple relevant pathways through which cloudiness and sea ice feed back on Earth's  
437 climate system (Solomon, S., D. Qin, M. Manning, Z. Chen, M. Marquis, K. B. Averyt, et al. 2007).  
438 Our evidence derived from Earth observations provides additional insight into the coupled  
439 radiative impacts of polar clouds and the changing sea ice cover (Fig. 8) that may provide a useful  
440 constraint on model projections and ultimately improve our understanding of present and future  
441 polar climate. ~~At the very least~~ On a practical level, our results demonstrate a simple correlation  
442 analysis between the net surface radiation budget and individual radiation budget terms that can  
443 be used to quickly evaluate climate models for realistic surface radiation budget variability in polar  
444 regions. Ultimately, our findings on the interplay between cloud and sea ice may support an  
445 improvement in the model representation of the cloud-ice interactions, mechanisms that may  
446 substantially affect the speed of the polar sea ice retreat, which in turn has a broad impact on the  
447 climate system, on the Arctic environment and on potential economic activities in the Arctic region  
448 (Buixadé Farré et al., 2014).



450 **Figure 9** Time series of the anomaly with respect to the whole period 1850-2100 of the radiative  
 451 flux. Mean modeled SWcre, LWcre and NETcre (blue) and surface SWsfc, LWsfc and NETsfc  
 452 (orange) anomalies over the 1850-2100 period under RCP8.5 scenario averaged over the Arctic  
 453 Ocean sea. The solid line shows the median, where the envelope represents the 25 and 75 percentile  
 454 of the 32 CMIP5 models. The linear regression (grey solid line and its 68% (dark grey envelope)  
 455 and 95% (light grey envelope) confidence interval) between: the trend in SWdown and trend in  
 456 sea ice extent (g and h); of the 32 CMIP5 climate models shown by grey dots over 2001-2016. The  
 457 observed trends are shown by red colors where confidence interval refers to standard error of the  
 458 trend.

459  
 460  
 461  
 462

463 **Acknowledgments:** The authors acknowledge the use of Clouds and the Earth's Radiant Energy  
464 System (CERES) satellite data version 4.0 from <https://ceres.larc.nasa.gov/index.php>, sea ice  
465 concentration data from National Snow and Ice Data Center (NSIDC) <http://nsidc.org/data/G02202>, as  
466 well as the modeling groups that contributed to the CMIP5 data archive at PCMDI  
467 <https://cmip.llnl.gov/cmip5/>.

468  
469 **Author Contributions:** RA ~~directed the study designed with contributions from all authors. RA the study~~  
470 ~~and~~ performed the analysis. ~~RA, AC, PCT and LGS contributed to the interpretation of the results.~~ RA,  
471 PCT, AC and GD drafted the paper. All authors commented on the text.

472 **Competing interests:** The authors declare no competing financial interests.

473 **Additional information:** The programs used to generate all the results are made with Python.  
474 Analysis scripts are available by request to R. Alkama.

#### 475 **References:**

476  
477 Abe, M., Nozawa, T., Ogura, T. and Takata, K.: Effect of retreating sea ice on Arctic cloud cover  
478 in simulated recent global warming, *Atmos. Chem. Phys.*, 16, 14343–14356, doi:10.5194/acp-16-  
479 14343-2016, 2016.

480  
481 Arzel, O., Fichefet, T. and Goosse, H.: Sea ice evolution over the 20th and 21st centuries as  
482 simulated by current AOGCMs, *Ocean Model.*, 12(3-4), 401–415,  
483 doi:10.1016/J.OCEMOD.2005.08.002, 2006.

484  
485 [Boeke, R. C. and P. C. Taylor: Seasonal energy exchange in sea ice retreat regions contributes to](#)  
486 [differences in projected Arctic warming. \*Nature Comm.\*, 9, 5017, doi: 10.1038/s41467-018-](#)  
487 [07061-9, 2018.](#)

488  
489 Boeke, R. C. and P. C. Taylor: Evaluation of the Arctic surface radiation budget in CMIP5  
490 models. *J. Geophys. Res.*, 121, 8525-8548, doi: 10.1002/2016JD025099, 2016.

491  
492 Boisvert, L. N. and Stroeve, J. C.: The Arctic is becoming warmer and wetter as revealed by the  
493 Atmospheric Infrared Sounder, *Geophys. Res. Lett.*, 42(11), 4439–4446,  
494 doi:10.1002/2015GL063775, 2015.

495  
496 Buixadé Farré, A., Stephenson, S. R., Chen, L., Czub, M., Dai, Y., Demchev, D., Efimov, Y.,  
497 Graczyk, P., Grythe, H., Keil, K., Kivekäs, N., Kumar, N., Liu, N., Matelenok, I., Myksovoll, M.,  
498 O’Leary, D., Olsen, J., Pavithran.A.P., S., Petersen, E., Raspotnik, A., Ryzhov, I., Solski, J., Suo,  
499 L., Troein, C., Valeeva, V., van Rijckevorsel, J. and Wighting, J.: Commercial Arctic shipping  
500 through the Northeast Passage: routes, resources, governance, technology, and infrastructure,  
501 *Polar Geogr.*, 37(4), 298–324, doi:10.1080/1088937X.2014.965769, 2014.

502  
503 Cesana, G., J. E. Kay, H. Chepfer, J. M. English, and G. de Boer: Ubiquitous low-level liquid-



504 containing Arctic clouds: New observations and climate model constraints from CALIPSO-  
505 GOCCP, *Geophys. Res. Lett.*, 39, L20804, doi:10.1029/2012GL053385, 2012.  
506

507 Charlock, T. P. and Ramanathan, V.: The Albedo Field and Cloud Radiative Forcing Produced  
508 by a General Circulation Model with Internally Generated Cloud Optics, *J. Atmos. Sci.*, 42(13),  
509 1408–1429, doi:10.1175/1520-0469(1985)042<1408:TAFACR>2.0.CO;2, 1985.  
510

511 Cheung, W. W. L., Lam, V. W. Y., Sarmiento, J. L., Kearney, K., Watson, R. and Pauly, D.:  
512 Projecting global marine biodiversity impacts under climate change scenarios, *Fish Fish.*, 10(3),  
513 235–251, doi:10.1111/j.1467-2979.2008.00315.x, 2009.  
514

515 Christensen, M., A. Behrangi, T. L'Ecuyer, N. Wood, M. Lebsock, and G. Stephens: Arctic  
516 observation and reanalysis integrated system: A new data product for validation and climate study,  
517 *Bull. Am. Meteorol. Soc.*, doi:10.1175/BAMS-D-14-00273.1, 2016.

518

519 Cohen, J., Screen, J. A., Furtado, J. C., Barlow, M., Whittleston, D., Coumou, D., Francis, J.,  
520 Dethloff, K., Entekhabi, D., Overland, J. and Jones, J.: Recent Arctic amplification and extreme  
521 mid-latitude weather, *Nat. Geosci.*, 7(9), 627–637, doi:10.1038/ngeo2234, 2014.  
522

523 Cohen, J., Zhang, X., Francis, J. *et al.* Divergent consensus on Arctic amplification influence  
524 on midlatitude severe winter weather. *Nat. Clim. Chang.* **10**, 20–29 (2020).  
525 <https://doi.org/10.1038/s41558-019-0662-y>, 2019.

526

527 Comiso, J. C., Parkinson, C. L., Gersten, R., Stock, L.: Accelerated decline in the arctic sea ice  
528 cover, *Geophys. Res. Lett.* <http://citeseerx.ist.psu.edu/viewdoc/summary?doi=10.1.1.419.8464>,  
529 2008.  
530

531 Curry, J. A., Schramm, J. L., Rossow, W. B. and Randall, D.: Overview of Arctic Cloud and  
532 Radiation Characteristics, *J. Climate*, 9(8), 1731–1764, doi:10.1175/1520-  
533 0442(1996)009<1731:OOACAR>2.0.CO;2, 1996.  
534

535 Duncan, B. N., Ott, L. E., Abshire, J. B., Brucker, L., Carroll, M. L., Carton, J. and  
536 coauthors: Space-based observations for understanding changes in the arctic-boreal  
537 zone. *Reviews of Geophysics*, 58, e2019RG000652. <https://doi.org/10.1029/2019RG000652>,  
538 2020.  
539

540 Graverson, R. G., Mauritsen, T., Tjernström, M., Källén, E. and Svensson, G.: Vertical structure  
541 of recent Arctic warming, *Nature*, 451(7174), 53–56, doi:10.1038/nature06502, 2008.  
542

543 Harrison, E. F., Minnis, P., Barkstrom, B. R., Ramanathan, V., Cess, R. D. and Gibson, G. G.:  
544 Seasonal variation of cloud radiative forcing derived from the Earth Radiation Budget  
545 Experiment, *J. Geophys. Res.*, 95(D11), 18687, doi:10.1029/JD095iD11p18687, 1990.  
546

547 Holland, M. M., Landrum, L., Raphael, M. and Stammerjohn, S.: Springtime winds drive Ross  
548 Sea ice variability and change in the following autumn, *Nat. Commun.*, 8(1), 731,



549 doi:10.1038/s41467-017-00820-0, 2017.  
550  
551 [Holland MM, Landrum L Factors affecting projected Arctic surface shortwave heating and](#)  
552 [albedo change in coupled climate models. \*Phil. Trans. R. Soc. A\* 373: 20140162, 2015.](#)  
553 <http://dx.doi.org/10.1098/rsta.2014.0162>  
554  
555 Kato, E., Kinoshita, T., Ito, A., Kawamiya, M. and Yamagata, Y.: Evaluation of spatially explicit  
556 emission scenario of land-use change and biomass burning using a process-based  
557 biogeochemical model, *J. Land Use Sci.*, 8(1), 104–122, doi:10.1080/1747423X.2011.628705,  
558 2013.  
559  
560 Kay, J. E., and Gettelman, A. : Cloud influence on and response to seasonal Arctic sea ice loss, *J.*  
561 *Geophys. Res.*, 114, D18204, doi:10.1029/2009JD011773, 2009.  
562  
563 Kay, J. E., and T. L'Ecuyer: Observational constraints on Arctic Ocean clouds and radiative  
564 fluxes during the early 21st century, *J. Geophys. Res. Atmos.*, 118, 7219–7236,  
565 doi:10.1002/jgrd.50489, 2013.  
566  
567 Kay, J. E., T. L'Ecuyer, H. Chepfer, N. Loeb, A. Morrison, and G. Cesana: Recent advances in  
568 Arctic cloud and climate research, *Curr. Clim. Change Rep.*, 2, 159, doi:10.1007/s40641-016-  
569 0051-9. 2016.  
570  
571 Komurcu, M., T. Storelvmo, I. Tan, U. Lohmann, Y. Yun, J. E. Penner, Y. Wang, X. Liu, and T.  
572 Takemura: Intercomparison of the cloud water phase among global climate models, *J. Geophys.*  
573 *Res. Atmos.*, 119, 3372–3400, doi:10.1002/2013JD021119. 2014.  
574  
575 Liu, Y., Key, J. R., Liu, Z., Wang, X. and Vavrus, S. J.: A cloudier Arctic expected with  
576 diminishing sea ice, *Geophys. Res. Lett.*, 39(5), doi:10.1029/2012GL051251, 2012.  
577  
578 Loeb, N. G., Doelling, D. R., Wang, H., Su, W., Nguyen, C., Corbett, J. G., Liang, L., Mitrescu,  
579 C., Rose, F. G., Kato, S., Loeb, N. G., Doelling, D. R., Wang, H., Su, W., Nguyen, C., Corbett, J.  
580 G., Liang, L., Mitrescu, C., Rose, F. G. and Kato, S.: Clouds and the Earth's Radiant Energy  
581 System (CERES) Energy Balanced and Filled (EBAF) Top-of-Atmosphere (TOA) Edition-4.0  
582 Data Product, *J. Clim.*, 31(2), 895–918, doi:10.1175/JCLI-D-17-0208.1, 2018.  
583  
584 Loeb, N.G., H. Wang, F.G. Rose, S. Kato, W.L. Smith, and S. Sun-Mack: Decomposing  
585 Shortwave Top-of-Atmosphere and Surface Radiative Flux Variations in Terms of Surface and  
586 Atmospheric Contributions. *J. Climate*, **32**, 5003–5019, [https://doi.org/10.1175/JCLI-D-18-](https://doi.org/10.1175/JCLI-D-18-0826.1)  
587 [0826.1](https://doi.org/10.1175/JCLI-D-18-0826.1), 2019.  
588  
589 Morrison, A. L., Kay, J. E., Chepfer, H., Guzman, R. and Yettella, V.: Isolating the Liquid Cloud  
590 Response to Recent Arctic Sea Ice Variability Using Spaceborne Lidar Observations, *Journal of*  
*Geophysical Research: Atmospheres*, 123(1), 473–490, doi:10.1002/2017JD027248, 2018.  
591  
592 Peng, G., Meier, W. N., Scott, D. J. and Savoie, M. H.: A long-term and reproducible passive

593 microwave sea ice concentration data record for climate studies and monitoring, *Earth Syst. Sci.*  
594 *Data*, 5(2), 311–318, doi:10.5194/essd-5-311-2013, 2013.

595  
596 [Pithan, F. & Mauritsen, T.: Arctic amplification dominated by temperature feedbacks in](#)  
597 [contemporary climate models. \*Nature Geoscience\* 7, 181–184, 2014.](#)

598  
599 Post, E., Bhatt, U. S., Bitz, C. M., Brodie, J. F., Fulton, T. L., Hebblewhite, M., Kerby, J., Kutz,  
600 S. J., Stirling, I. and Walker, D. A.: Ecological consequences of sea-ice decline., *Science*,  
601 341(6145), 519–24, doi:10.1126/science.1235225, 2013.

602  
603 Qu, X. and A. Hall: Assessing snow albedo feedback in simulated climate change. *J.*  
604 *Climate*, 19(11), 2617–2630, 2006

605  
606 Ramanathan, V., Cess, R. D., Harrison, E. F., Minnis, P., Barkstrom, B. R., Ahmad, E. and  
607 Hartmann, D.: Cloud-radiative forcing and climate: results from the Earth radiation budget  
608 experiment., *Science* (80-. ), 243(4887), 57–63, doi:10.1126/science.243.4887.57, 1989.

609  
610 Serreze, M. C., Holland, M. M. and Stroeve, J.: Perspectives on the Arctic’s Shrinking Sea-Ice  
611 Cover, *Science* (80-. ), 315(5818), 1533–1536, doi:10.1126/science.1139426, 2007.

612  
613 Simmonds, I.: Comparing and contrasting the behaviour of Arctic and Antarctic sea ice over the  
614 35 year period 1979-2013, *Ann. Glaciol.*, 56(69), 18–28, doi:10.3189/2015AoG69A909, 2015.

615  
616 Sledd A. and L'Ecuyer T.: How Much Do Clouds Mask the Impacts of Arctic Sea Ice and Snow  
617 Cover Variations? Different Perspectives from Observations and Reanalyses. *Atmosphere*,  
618 10(1), 12; <https://doi.org/10.3390/atmos10010012>, 2019.

619  
620 Solomon, S., D. Qin, M. Manning, Z. Chen, M. Marquis, K.B. Averyt, M. T. and H. L. M.:  
621 Contribution of Working Group I to the Fourth Assessment Report of the Intergovernmental  
622 Panel on Climate Change, 2007.  
623 [http://www.ipcc.ch/publications\\_and\\_data/ar4/wg1/en/contents.html](http://www.ipcc.ch/publications_and_data/ar4/wg1/en/contents.html), 2007.

624  
625 Stroeve, J., Holland, M. M., Meier, W., Scambos, T. and Serreze, M.: Arctic sea ice decline:  
626 Faster than forecast, *Geophys. Res. Lett.*, 34(9), doi:10.1029/2007GL029703, 2007.

627  
628 [Stuecker, M. F. et al.: Polar amplification dominated by local forcing and feedbacks. \*Nature\*](#)  
629 [Climate Change](#) 8, 1076–1081, 2018.

630  
631 Taylor, K. E., Stouffer, R. J. and Meehl, G. A.: An Overview of CMIP5 and the Experiment  
632 Design, *Bull. Am. Meteorol. Soc.*, 93(4), 485–498, doi:10.1175/BAMS-D-11-00094.1, 2012.

633  
634 Taylor, P., Hegyi, B., Boeke, R. and Boisvert, L.: On the Increasing Importance of Air-Sea  
635 Exchanges in a Thawing Arctic: A Review, *Atmosphere* (Basel)., 9(2), 41,  
636 doi:10.3390/atmos9020041, 2018.

637

638 Taylor, P. C., Kato, S., Xu, K.-M. and Cai, M.: Covariance between Arctic sea ice and clouds  
639 within atmospheric state regimes at the satellite footprint level, *J. Geophys. Res. Atmos.*,  
640 120(24), 12656–12678, doi:10.1002/2015JD023520, 2015.

641

642 Trepte Q. Z. et al., "Global Cloud Detection for CERES Edition 4 Using Terra and Aqua MODIS  
643 Data," in *IEEE Transactions on Geoscience and Remote Sensing*, vol. 57, no. 11, pp. 9410-9449,  
644 Nov. 2019.

645

646 Turner, J., Bracegirdle, T. J., Phillips, T., Marshall, G. J., Hosking, J. S., Turner, J., Bracegirdle,  
647 T. J., Phillips, T., Marshall, G. J. and Hosking, J. S.: An Initial Assessment of Antarctic Sea Ice  
648 Extent in the CMIP5 Models, *J. Clim.*, 26(5), 1473–1484, doi:10.1175/JCLI-D-12-00068.1,  
649 2013.

650

651 Meier W., Fetterer, M. Savoie, S. Mallory, R. Duerr, and J. S.: NOAA/NSIDC Climate Data  
652 Record of Passive Microwave Sea Ice Concentration, Version 3. Boulder, Colorado USA.  
653 NSIDC: National Snow and Ice Data Center., doi:<https://doi.org/10.7265/N59P2ZTG>, 2017.

654

655 Zhang, X. and Walsh, J. E.: Toward a Seasonally Ice-Covered Arctic Ocean: Scenarios from the  
656 IPCC AR4 Model Simulations, *J. Clim.*